DYNAMIC AEROELASTIC INSTABILITIES OF AN AIRCRAFT WING WITH UNDERWING STORE IN TRANSONIC REGIME

CHAKRADHAR BYREDDY, RAMANA GRANDHI
Wright State University
Dayton, OH 45435

PHILIP BERAN
Multidisciplinary Technologies Center
AFRL, WPAFB, Dayton OH 45433

SUBMITTED TO
ACTA ASTRONAUTICA JOURNAL
MAY 2003

DYNAMIC AEROELASTIC INSTABILITIES OF AN AIRCRAFT WING WITH UNDERWING STORE IN TRANSONIC REGIME

Chakradhar Byreddy[*], *Ramana V. Grandhi*[**]

Department of Mechanical and Materials Engineering

Wright State University, Dayton, Ohio 45435

Philip Beran[†]

MultiDisciplinary Technologies Center

AFRL, Wright Patterson Air Force Base, Ohio 45433-7531

Abstract

The research used the Transonic Small Disturbance (TSD) theory to better understand the dynamic aeroelastic phenomena and factors that affect the onset of flutter and store induced Limit-Cycle Oscillations (LCO) in the transonic regime. Several parametric studies of the flutter and LCO of an aircraft wing with underwing store in the transonic regime were conducted, as well as an investigation of the effect of inclusion of store aerodynamics on the onset of flutter. The flutter sensitivity was analyzed for the following store parameters: (i) Location of underwing store center of gravity with respect to aerodynamic root chord. (ii) Location of underwing store along

---

* Graduate Research Assistant, E-mail address: cbyreddy@cs.wright.edu

** Distinguished Professor, Associate Fellow AIAA

† Principal Research Aerospace Engineer

the span of the wing and (iii) Underwing clearance (pylon length). Also, studies were conducted to identify the onset of LCO for different configurations of underwing store and flight regimes (unmatched analysis), thereby identifying the parameters that induce LCO. The sensitive parameters that affect flutter and LCO are identified.

1. Introduction

Many fighter aircraft carry out their missions in the transonic regime, and the presence of external stores pose complex and dangerous problems in this regime. In transonic flow regimes, the effect of aerodynamic nonlinearities becomes significant due to the presence of shocks on the wing surface, and dynamic aeroelastic instabilities such as flutter and LCO are induced due to the presence of external stores. A computational method based on the inviscid Transonic Small Disturbance Theory is used to predict the nonlinear unsteady aerodynamics associated with shock motions in the transonic flow region [1]. This method is used to solve the nonlinear governing equations in aeroelastic analysis, and provides an efficient but accurate alternative to linear method such as the doublet lattice method (panel method).

Previous literature helped in understanding the implications of an aircraft wing with external stores (stores considered as rigid bodies) on the static aeroelastic phenomena and unsteady pressure distributions in the transonic regime [2]. Also, some work has been performed on the LCO of an aircraft wing, but not on the parameters of underwing store affecting the dynamic aeroelastic phenomena in the transonic regime. The present work advances the ongoing research that is being performed at the Air Force Research Laboratory (AFRL) by investigating the effects of dynamic aeroelastic phenomena taking place in flight vehicles carrying stores (missiles, launchers, fuel tanks,

etc.) [3]. In the present work, different underwing store configurations were chosen so as to understand the influence of the structural parameters of store on the dynamic aeroelastic instabilities. Presence of underwing stores causes flutter and store induced LCO in the transonic regime, which can lead to several problems associated with target-locking system, roll maneuverability etc. Therefore, it plays an important role in the preliminary design stage.

The research work has been divided into two phases. The first phase involves the validation of computation of flutter by conducting analysis on a clean wing (i.e., one without store) using Automated Structural Optimization System (ASTROS) [4] and Computational Aeroelasticity Program Transonic Small Disturbance (CAP-TSD) (linear and nonlinear analysis) in the subsonic regime. One of the core issues during the analysis of flutter and LCO behavior is the inclusion of store aerodynamics [5]. The second phase of the work involves an investigation of the effect of variation in the store parameters such as the underwing store center of gravity, underwing store location along the span of the wing and underwing clearance in the transonic region. These parametric studies are conducted by considering the underwing store mass only and underwing store aerodynamics. The accuracy of computed flutter velocity is compared in both cases to understand the impact of inclusion of store aerodynamics. Thus, identifying whether the effect of store aerodynamics has to be included or neglected in the optimization algorithms (which are iterative in nature). These analyses also help in identifying the critical parameters that directly affect the flutter and LCO in the transonic region. By obtaining the sensitivities of these parameters to flutter and LCO, least sensitive

parameters can be ignored in the analysis, resulting in reduced computational time and costs.

With the results obtained from the second phase, it is viable to incorporate nonlinear analysis into the preliminary design process. Based on the information obtained from the above analyses, a multidisciplinary optimization methodology could be developed to design a wing structure with external stores to delay the occurrence of dynamic aeroelastic phenomena such as flutter and LCO. The information obtained from this work will facilitate in simulation based store certification in the transonic regime. Thereby significantly reducing the number of expensive and extensive flight tests for store certification.

2. Motivation and Benefits

Many problems associated with fluid-structure interaction are quite complicated, particularly that of wing-store interaction. Different research approaches have been extensively studied and developed in order to understand the impact of structures and aerodynamics associated with wing and store. High computing power led to the advent of various numerical methods to solve the aeroelastic problems for application to realistic aircraft configurations in the transonic regime such as CAP-TSD [6]. Also, most of the research work for wing-body configuration was carried out in either subsonic or supersonic flow regimes [7]. The influence of store aerodynamics on different wing configurations have been studied, and the results have been compared with present flight flutter data [8]. A considerable amount of work has been conducted on the preliminary design for aircraft structures for improved control effectiveness (steady state roll performance) in the transonic region [9]. A methodology was also developed and

compared with flutter flight test data for including transonic flutter requirements for preliminary automated structural design of a clean wing [10]. The various factors that affect LCO have been extensively studied [11] by considering the structural nonlinearities as well as aerodynamic nonlinearities of a wing with tip store. The current work involves a comprehensive parametric study of underwing store on flutter and LCO by using various nonlinear analysis tools. In the present research a design methodology is developed by integrating various tools associated with nonlinear analysis for improved air vehicles with external stores in the transonic regime. This work can be advanced by including the effects of pylon stiffness [12], i.e., various types of attachments and also the flutter of store itself. The flutter of store itself might cause extensive fatigue to the pylon. Therefore studies involving all these effects help in better understanding the mechanisms and physical significance that govern the onset of flutter and LCO due to the presence of underwing stores. Also, the optimization of critical store structural parameters helps in increasing the air vehicle life, performance and flight envelope during their mission. Thus, it helps in the study of the preliminary design of aircraft structures with and without stores for improved flutter and LCO performance in the transonic regime.

3. Governing Equations

The TSD theory is based on the assumption that in the transonic flow regime, there are small disturbances, or perturbations around, a thin wing. The TSD equation in conservation form is given as

$$\frac{\partial}{\partial t}(-A\phi_t - B\phi_x) + \frac{\partial}{\partial x}(E\phi_x + F\phi^2{}_x + G\phi^2{}_y) + \frac{\partial}{\partial y}(\phi_y + H\phi_x\phi_y) + \frac{\partial}{\partial z}(\phi_z) = 0 \qquad (1)$$

where ϕ is the inviscid small disturbance velocity potential. It is the nonlinearity in ϕ that helps in modeling weak shock waves in the transonic regime. In the analyses only, two different forms of the TSD equation are used by choosing either the linear equation coefficients or the AMES coefficients. The coefficients A, B, E, are

$$A = 2M_\infty^2 \tag{2}$$

$$B = 2M_\infty^2 \tag{3}$$

$$E = 1 - M_\infty^2 \tag{4}$$

where M_∞ the free stream Mach number and γ is is the ratio of specific heats. The value of γ used in these analyses is 1.4 (air). The coefficients F, G and H are called AMES coefficients, given as

$$F = -1/2(\gamma+1)M_\infty^2 \tag{5}$$

$$G = -1/2(\gamma-3)M_\infty^2 \tag{6}$$

$$H = -(\gamma-1)M_\infty^2 \tag{7}$$

The nonlinear results are computed by using the AMES coefficients given by the equation

$$\frac{\partial}{\partial t}(-M_\infty^2\phi_t - 2M_\infty^2\phi_x) + \frac{\partial}{\partial x}((1-M_\infty^2)\phi_x - \frac{1}{2}(\gamma+1)M_\infty^2\phi_x + \frac{1}{2}(\gamma-3)M_\infty^2\phi^2{}_y) + \frac{\partial}{\partial y}(\phi_y(1-(\gamma-1)$$
$$M_\infty^2\phi_x)) + \frac{\partial}{\partial z}(\phi_z) = 0 \tag{8}$$

The linear results are computed by setting the coefficients given by the equation

$$\frac{\partial}{\partial t}(-M_\infty^2\phi_t - 2M_\infty^2\phi_x) + \frac{\partial}{\partial x}((1-M_\infty^2)\phi_x) + \frac{\partial}{\partial y}(\phi_y) + \frac{\partial}{\partial z}(\phi_z) = 0 \tag{9}$$

When the linear equation was used, the wing and store was modeled as a flat plate in order to produce results similar to other methods such as the doublet-lattice method.

When the nonlinear equation was used, the wing was modeled using an appropriate airfoil such as NACA0004, (zero camber, symmetric and four percent thick) so that the nonlinear effects (such as moving shock waves) can be realistically captured. However the store is modeled as a flat plate, for inclusion of store aerodynamics. Coupling of the structural equations of motion with the unsteady aerodynamics of wing and store is implemented and only the vertical component of the mode shape is used for both the wing and store.

4. Analysis Methodology

The CAP-TSD code solves the unsteady transonic small disturbance equation using an implicit time–accurate approximate factorization algorithm [13]. The unsteady aerodynamics is simultaneously integrated with the structural equation of motions in time. For this the vibration analysis is performed using ASTROS [14] and the displacements are splined on to the CAP-TSD grid of the wing using a Thin Infinite Plane Spline (IPS) [15]. This integration is represented by the structural response in time to some initial perturbations. The structure is modeled by a series of orthogonal mode shapes weighted with time varying coefficients called the generalized displacements. The generalized coordinate transformation represents the physical deformations of the structure. The modal deflections in the streamwise and spanwise directions are minute in comparison to the vertical modal displacements, and thus, neglected. Therefore, the position of the wing at any point in time is given as

$$z_i(x,y,t) = \sum_{i=1}^{ModeNumber} u_i f_i(x,y) \qquad (10)$$

where u_i is the time varying generalized displacements and f_i represents the vertical components of the mode shapes. The structural equations of motion in generalized coordinates are given as

$$M\ddot{u} + B\dot{u} + Ku = F \qquad (11)$$

K- Structural Stiffness

B- Structural Damping

M- Structural Mass

F- External aerodynamic loads

where $$F = \rho_\infty u_\infty^2 \frac{c_r^2}{2} \int_s z_i \frac{\Delta p}{\rho_\infty u_\infty^2 \frac{c_r^2}{2}} ds \qquad (12)$$

ρ_∞ - Free stream density

c_r - Wing reference chord

u_∞ - Free stream velocity

Δp - Lifting pressure

z_i - Mode shape described in equation 10

Equation 11 is solved with equation 8 by using an implicit time-marching aeroelastic solution procedure based on approximate factorization [16]. In the current work, the procedure for the assessment of flutter prediction is described using the flow chart in Fig 1. In this method, the flutter velocity is calculated by varying free stream velocity and dynamic pressure ($q = \frac{1}{2}\rho u_\infty^2$) while holding the density constant at a given Mach number (which is called an unmatched analysis). To compute the point at which flutter

first occurs for a given Mach number, several executions of the CAP-TSD code are required at different dynamic pressures. All CAP-TSD calculations include the effects of shock generated entropy and vorticity. A static aeroelastic analysis is performed at a given dynamic pressure (that is assumed to be near neutral stability) to create a steady flow field that reflects the wing thickness, camber and mean angle of attack. This steady flow field is essential for the proper computing of the free decay transients in the dynamic aeroelastic analysis. If the static aeroelastic solution is converged, then the dynamic aeroelastic analysis is performed by restarting the calculation from the converged static aeroelastic solution with some initial disturbance on the vertical velocity of the wing. If the solution is not converged, then the number of iterations is increased till the static solution converges. After the dynamic analysis is run, the stability of the system (coefficient of lift) is determined. If the system is stable, the entire procedure is repeated by increasing the dynamic pressure; else the damping value is computed. The flutter dynamic pressure value is determined by linearly extrapolating the damping information using the logarithmic decrement method [17]. Moreover, further refinement of the damping can be obtained by additional aeroelastic analyses if improved accuracy of flutter velocity is desired.

5. Computational Models

5.1. Structural modeling of Wing and Underwing store

Fig 2 represents the structural model of wing and store. A wing model called the Intermediate Complexity Wing (ICW2001), which has characteristics of a conventional fighter aircraft, is chosen for the study of wing-store interaction. The ICW2001 is modeled using 199 elements. In this model, 80 membrane elements with bending

capability are used to represent the wing skins, 70 shear panels represent the spars and ribs, and 49 rod elements represent the posts. The wing skin is modeled using QUAD4 and TRIA3 elements in ASTROS. SHEAR elements are used for modeling the spars and ribs. ROD elements are used for modeling the posts. The wing root is fully constrained by using single point constraints. The following are the characteristics of ICW2001:

- Configuration
  - Thickness of the wing section: A constant thickness of four percent is maintained through out the span in order to have a NACA0004 airfoil [18].
  - Extension of wing tip: The span of the wing model is extended to 108 inches, in case of attachment of tip store and for further analysis for multiple store configurations.
- Structural mass of wing
  - 98 pounds
- Non structural mass of wing
  - 327 pounds

The ratio of structural mass to non-structural mass is 0.3 and angle of sweep is 22.61^0. The lengths of the root and tip chord are 48 and 26 inches respectively. The material used for modeling the wing is Aluminum (AL-7050-T7451) with E = 10.3 x 10^6 psi. Since the skin of wing is modeled with bending capability, the store connections (pylon) are modeled as BAR elements, with high stiffness (E = 30 x 10^6 psi) to represent a rigid body. The pylon mass is 114.7 lb. The connections are modeled in the form of V shape. The store is modeled with BAR elements. The material properties of the store are E =

10.3×10^6 psi and specific weight = 0.3 lb/in^3. Mass of store with non-structural mass is 185.2 lb. The store configuration properties are presented in Table 1. The percentage of store mass to wing mass is 44 percent. Each configuration has a different center of gravity. The center of gravity is varied by changing the non structural mass distribution on the nodes of the store. We chose these configurations so as to understand the impact of position of various guidance systems, warheads, etc. on the underwing store.

5.2. Aerodynamic modeling of Wing and Underwing store using CAP-TSD

Fig 3 represents the aerodynamic model of wing with store. The dimension for this computational grid is 90 x 30 x 60. The actual aerodynamic model of wing with root and tip chord is 90 and 48 inches respectively. This aerodynamic model is normalized to the computational grid which represents the physical region of the wing (schematically represented as a horizontal lifting surface in solid green lines). The dimension of the computational grid representing the wing is 50 x 15. Similarly the aerodynamic model of the store with the chord length 90 inches is normalized to the computational grid which represents the physical region of the store (second horizontal lifting surface in solid green lines). Even though the store planform in CAP-TSD grid is not rectangular it primarily helps in understanding the significance of store aerodynamics on the dynamic aeroelastic instabilities. The dimension of the computational grid representing the store is 56 x 2. The transformation region is defined in order to relate the computational grid and physical region. In this modeling, the effect of the vertical lifting surface (pylon) is neglected.

6. Results and Discussions

This section discusses the numerical results obtained for the intermediate complexity wing and also wing with underwing store. Prior to making numerous aeroelastic calculations, a convergence study was done to show that the time step (Δt = 0.05 and 0.02 seconds) and grid dimensions (90 x 30 60 and 120 x 60 x 90) had no effect on the CAP-TSD aeroelastic solutions. Also, each dynamic solution is computed by using the converged static solution with some form of initial condition for the generalized displacements or velocities for each structural mode. A small initial perturbation is created by giving a value of one to generalized velocities for each mode in all the dynamic aeroelastic calculations ($\dot{u}_i$ = 1.0, i = 1, 6) to initiate the motion of the wing. Also, the initial conditions on the generalized displacements of each mode are taken to be zero to reduce the numerical transients and corresponding instabilities. Sensitivity of aeroelastic solutions to the initial conditions is also verified. The choice of using an initial generalized velocity of one is arbitrary and its effect on the structural response depends on how the mode shapes are scaled [19]. Finally, dynamic aeroelastic results are presented for the following cases.

Case I: *Clean wing*

Case II: *Wing with underwing store (Mass only) and*

Case III: *Wing with underwing store (Store aerodynamics included)*

Case I constitutes the first phase, and Case II and Case III constitutes the second phase of the research work. Several flutter points were computed with CAP-TSD using the linear (to compare with ASTROS) and nonlinear equations. For all sets of results, the flutter points were computed by holding the density constant and varying the velocity, as

described above. No structural damping was used, and all the calculations were performed with wing root set at zero angle of attack.

Case I: This work helps to validate the CAP-TSD analysis conducted on a clean wing. Fig 4 shows that the CAP-TSD linear results at low Mach numbers are in excellent agreement with ASTROS. The good agreement between CAP-TSD linear and ASTROS at low Mach numbers should be expected, since nonlinear aerodynamic effects there are insignificant. Fig 4 also shows the nonlinear results in comparison with linear results. Nonlinearities do not become significant until Mach 0.8, leading to the presence of a transonic dip at Mach number 0.9 due to the effect of shocks. The large differences between the results using linear and nonlinear equations in the transonic region are due to the presence of shocks in the flow field, as shown in Fig 5 for Mach 0.90 and 0.92 respectively.

Case II: The various store configurations used have their center of gravity at 22, 44 and 66 percent of the aerodynamic chord, respectively, as shown in Fig 6. Fig 7 shows the sensitivity of flutter to location of store center of gravity. The results indicate that the flutter velocity of the aircraft wing with underwing store increases, a favorable change, if the underwing store center of gravity is forward of the elastic axis of the wing. The extent to which the store can be moved forward depends on the design constraints of the store parameters. Also, there is a shift of transonic dip from Mach number 0.90 to 0.92 due to the presence of store. Fig 8 shows the sensitivity of flutter with location of the store along the span of the wing. The results indicate that as the store is located near the aerodynamic root chord the flutter velocity increases, thereby indicating that underwing stores can be placed near the fuselage in order to delay the occurrence of flutter. Fig 9 shows the

sensitivity of flutter with underwing clearance. The results indicate that as the underwing clearance increases, the flutter velocity decreases, due to the structural deformations associated with the pylon. Even though the pylon is realistically stiff, these deformations are dominant over the aerodynamic interference effects between the store and pylon (inclusion of pylon aerodynamics using panel method does not have any significant change in flutter velocity but change in the structural properties of pylon has significant effect. Thus, the same can be attributed to the nonlinear region since it is mass only aerodynamics). Also, there is a significant decrease in the first bending and torsion modal frequencies (shown in Table 2) with the increase in the underwing clearance, thereby indicating that the flutter velocity will be decreased with increase in underwing clearance. Fig 10 shows the sensitivity of flutter with location of store (for various store configurations) along the span, which indicates that the presence of store center of gravity at fore of the elastic axis increases the flutter velocity. Similarly, Fig 11 shows the sensitivity of flutter with underwing clearance (for various store configurations), which also supports the conclusion that as underwing clearance increases the flutter velocity decreases. There was no presence of LCO for different wing-store configurations at various Mach numbers with mass only aerodynamics.

Case III: Fig 12 shows a three-dimensional view of the aerodynamic model using CAP-TSD. Here the underwing store is modeled as a horizontal lifting surface. Splining of displacements on to the aerodynamic grid of the underwing store was done by considering the relative displacements of the underwing store with the wing. The splined displacements of the wing enclosing the store region are extrapolated on to the grid of the underwing store, as shown in Fig 4. Fig 13 and Fig 14 show that the inclusion of store

aerodynamics in the transonic regime does not have any significant effect in the case of wing-store configuration 2. Fig 15 shows that for store configuration 2 at Mach 0.94, the flutter velocity was more for wing with store (aerodynamics) than with the wing and store (mass only), but the flutter velocity is same with store aerodynamics and store (mass only) for store configuration 1. Another interesting observation made was that the flutter velocity is more at Mach 0.94 than at Mach 0.90 with inclusion of store aerodynamics for the store configuration 2, but it is different in case of store configuration 1. Store configuration 1 shows greater sensitivity to store aerodynamics, reducing onset flutter speed by 10 percent (approximately) at Mach 0.90. Thus, from the analyses we can conclude which wing-store configurations have significant impact on flutter with inclusion of store aerodynamics at various Mach numbers. Also, no LCO was found for different wing-store configurations at various Mach numbers with inclusion of store aerodynamics.

7. Summary Remarks

Underwing stores have a major effect on the dynamic aeroelastic instabilities of a wing, both structurally and aerodynamically. Underwing stores reduce the natural frequencies because of its inertia effect. Also it reduces the flutter velocity depending on where it is located with respect to the elastic axis of the wing. The flutter speed increases as the underwing store center of gravity is moved forward of elastic axis and decreases when moved aft. Also the flutter velocity increases as the underwing store is moved towards the aerodynamic root chord. Flutter velocity also decreases as the underwing store clearance (pylon length) is increased. Thus, the store structural parameters affecting the dynamic aeroelastic phenomena are investigated. Further investigations are done to

predict the onset and severity of store induced flutter and LCO by including the underwing store aerodynamics. The results indicated that inclusion of store aerodynamics for the wing with these underwing store configurations does not make any significant effect on the dynamic aeroelastic phenomena in the transonic regime.

8. Acknowledgement

This research work has been sponsored by Air Force Office of Scientific Research (AFOSR) through the grant number F49620-01-1-0179. The authors would like to thank Dr. Frank Eastep, Dr. Brian Sanders and Dr. Narendra Khot of Wright Patterson Air Force Base, OH, for their valuable suggestions. The authors would also like to thank Dr. John Edwards and Dr. David Schuster of NASA Langley, Hampton, VA, for providing the CAP-TSD program.

9. Bibliography

1. Batina, J. T., "Efficient Algorithm for Solution of the Unsteady Transonic Small – Disturbance Equation", *Journal of Aircraft*, Vol.23, July 1988, pp. 598-605.

2. Batina, J.T., Seidal, D.A., Bland, S.R. and Bennett, R.M., "Unsteady Transonic Flow Calculations for Realistic Aircraft Configurations, AIAA Paper no. 87-0850, Presented at the AIAA/ASME/ASCE/AHS 28th Structures, Structural Dynamics and Materials Conference, Monterey, CA, April 2-4, 1990.

3. Beran, P.S, Khot, N.S., Eastep, F.E., Snyder, R.D., Zweber, J.V., Huttsell, L.J., Scott, J.N., "The Dependence of Store-Induced Limit-Cycle Oscillation Predictions on Modeling Fidelity", Proceedings of the RTO Applied Vehicle Technology Panel Symposium on "Reduction of Military Vehicle Acquisition Time and Cost Through

Advanced Modeling and Virtual Product Simulation," Paris, France, 22-25 April, 2002, paper #44.

4. Johnson E., and Venkayya V.B., "Automated Structural Optimization System (ASTROS)", Volume-I Theoretical Manual, U.S. Air Force Wright Aeronautical Labs., TR-88-3028 (1988).

5. Turner, C.D., "Effect of Store Aerodynamics on Wing/Store Flutter", *Journal of Aircraft*, Vol. 19, July 1982, pp. 574-580.

6. Batina, J. T., "Unsteady Transonic Flow Calculations for Wing-Fuselage Configurations", *Journal of Aircraft*, Vol.23, Dec. 1986, pp. 897-903.

7. Van Zyl, L.H., "Modelling of Wing-Body Combinations in Unsteady Supersonic Flow", Proceedings of the International Forum on Aeroelasticity and Structural Dynamics 1993, Volume 1, pp. 189-204.

8. Chen, P.C., Sulaeman, E., Liu, D.D., and Denegri Jr. C.M., "Influence of External Store Aerodynamics on Flutter/LCO of a Fighter Aircraft", AIAA Paper 2001-1410.

9. Aryasomayajula, R., "Multidisciplinary Design of Vehicle Structures with Improved Roll Maneuverability", Master's Thesis, Department of Mechanical and Materials Engineering, Wright State University.

10. Kolonay, R., "Unsteady Aeroelastic Optimization in the Transonic Regime", Doctor of Philosophy Thesis, School of Aeronautics and Astronautics, Purdue University.

11. Kim, Kiun, and Strganac, T.W., "Aeroelastic studies of a cantilever wing with structural and aerodynamic nonlinearities.", 43rd AIAA/ASME/ASCE/AHS/ASC

Structures, Structural Dynamics and Materials Conference, April 22-25, 2002, Denver, Colorado, AIAA-2002-1412.

12. Desmarias, R.N., Reed III, W.H., "Wing/store flutter with nonlinear pylon stiffness", *Journal of Aircraft*, Vol. 18, 1980, pp. 984-987.

13. Batina, J. T., "Unsteady Transonic Algorithm Improvements for Realistic Aircraft Configurations", *Journal of Aircraft*, Vol.26, Feb 1989, pp. 131-139.

14. Karpel, M., "Efficient Vibration Mode Analysis of Aircraft with Multiple External Store Configurations", *Journal of Aircraft*, Vol.25, Aug. 1988, pp. 747-751.

15. ASTROS Version 13 and ESHELL Users Manual, Universal Analytics, Inc., Torrance, CA.

16. Edwards, J.W., Bennett, R.M., Whitlow, W., Jr., Seidel, D.A., "Time Marching Transonic Flutter Solutions Including Angle-of-Attack Effects", 23rd AIAA/ASME/ASCE/AHS/ASC Structures, Structural Dynamics and Materials Conference, New Orleans, Louisiana, AIAA paper no. 82-3685.

17. Jennifer, H., "Analytical and Experimental Investigation of Flutter Suppression by Piezoelectric Actuation", NASA Technical Paper 3241, Appendix E, Feb 1993.

18. Jun, S., Tischler, V.A. and Venkayya, V.B. (2002). "Multidisciplinary design optimization of a built-up wing structure with tip missile", 43rd AIAA/ASME/ASCE/AHS/ASC Structures, Structural Dynamics and Materials Conference, April 22-25, 2002, Denver, Colorado, AIAA-2002-1421.

19. Gibbons Michael D., "Aeroelastic Calculations Using CFD for a Typical Business Jet Model", NASA CR 4753.

List of Tables and Figures

Figure 13: Comparison of Flutter velocities for Linear (ASTROS), Linear (CAP-TSD) and Non-Linear (CAP-TSD) for store configuration 2

Figure 14: Comparison of flutter velocities (knots) for M=0.9 and M=0.92 using Non-Linear (CAP-TSD) for store configuration 2

Figure 15: Comparison of flutter for store configurations 1 and 2 with and without store aerodynamics

Configuration Number	Description of the store configuration	Type of Configuration	Properties of the Underwing store
Configuration 1	Store center of gravity at 22 percent, underwing clearance at 7.7 percent of aerodynamic root chord and store at 67 percent of aerodynamic span	Fore	Weight = 185.2 lbs Length = 80 inches Area Moments of Inertia = 14.86 in^4 Torsion Constant = 29.72 in^4
Configuration 2	Store center of gravity at 44 percent, underwing clearance at 7.7 percent of aerodynamic root chord and store at 67 percent of aerodynamic span	Near Elastic	Weight = 185.2 lbs Length = 80 inches Area Moments of Inertia = 14.86 in^4 Torsion Constant = 29.72 in^4
Configuration 3	Store center of gravity at 66 percent, underwing clearance at 7.7 percent of aerodynamic root chord and store at 67 percent of aerodynamic span	Aft	Weight = 185.2 lbs Length = 80 inches Area Moments of Inertia = 14.86 in^4 Torsion Constant = 29.72 in^4
Configuration 4	Store center of gravity at 44 percent, underwing clearance at 7.7 percent of aerodynamic root chord and store at 56 percent of aerodynamic span	Span	Weight = 185.2 lbs Length = 80 inches Area Moments of Inertia = 14.86 in^4 Torsion Constant = 29.72 in^4
Configuration 5	Store center of gravity at 44 percent, underwing clearance at 16.7 percent of aerodynamic root chord and store at 67 percent of aerodynamic span	pylon	Weight = 185.2 lbs Length = 80 inches Area Moments of Inertia = 14.86 in^4 Torsion Constant = 29.72 in^4

Table 1: Different store configurations

Mode Number	Modal Frequencies (Hz)					
	Clean Wing	Store Configuration 1	Store Configuration 2	Store Configuration 3	Store Configuration 4	Store Configuration 5
1	8.53	5.82	5.55	5.32	6.71	5.14
2	29.64	13.65	15.36	17.49	18.88	12.76
3	36.67	31.81	31.38	31.21	28.93	24.38
4	61.41	64.54	64.87	65.97	58.53	63.86

Table 2: Modal frequencies for different wing-store configurations

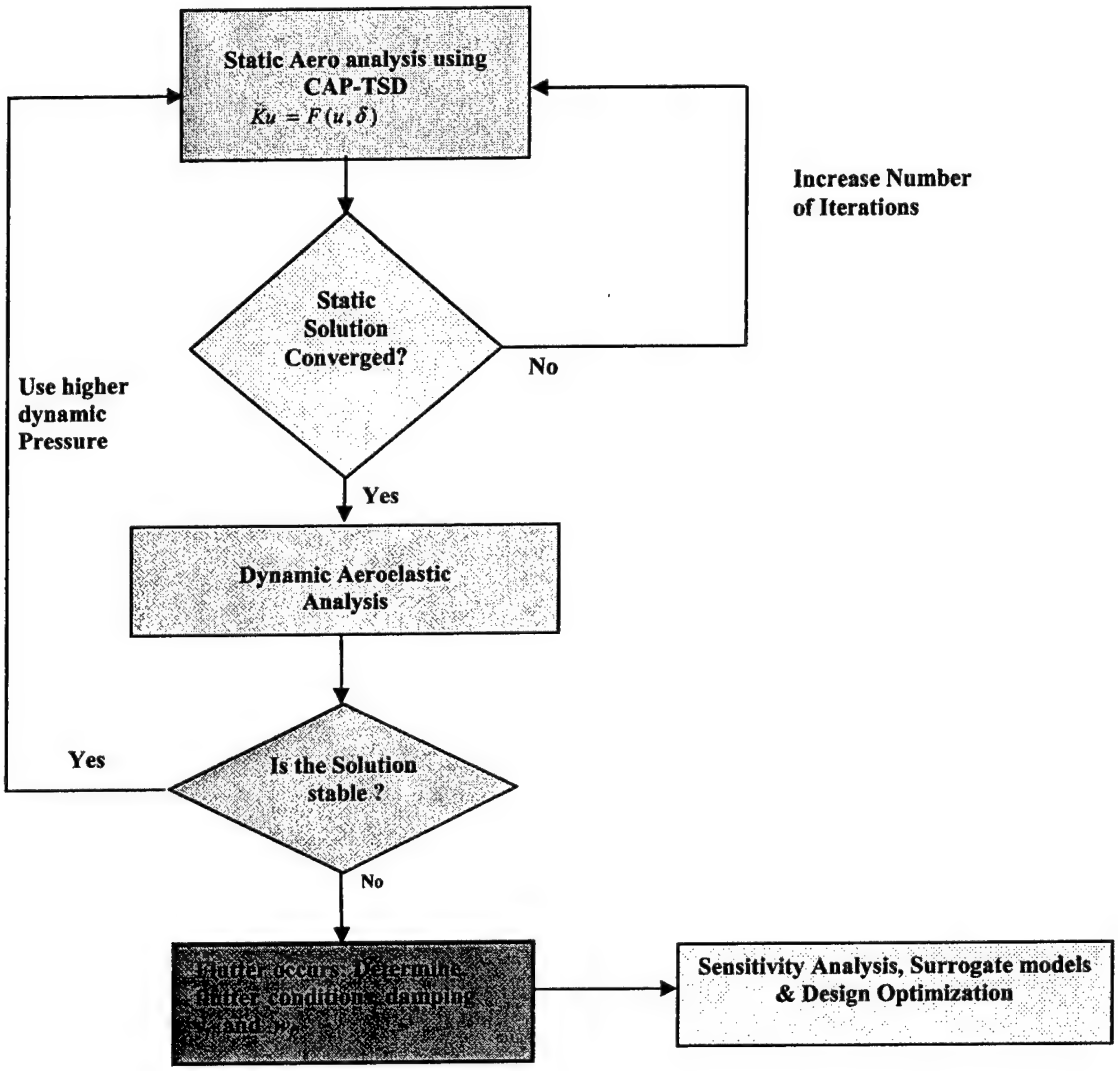

Figure 1: Flow chart for analysis methodology

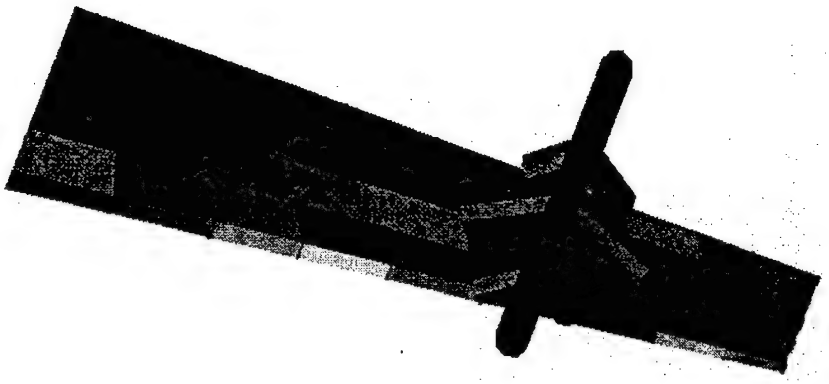

Figure 2: Modified Intermediate Complexity Wing with underwing store

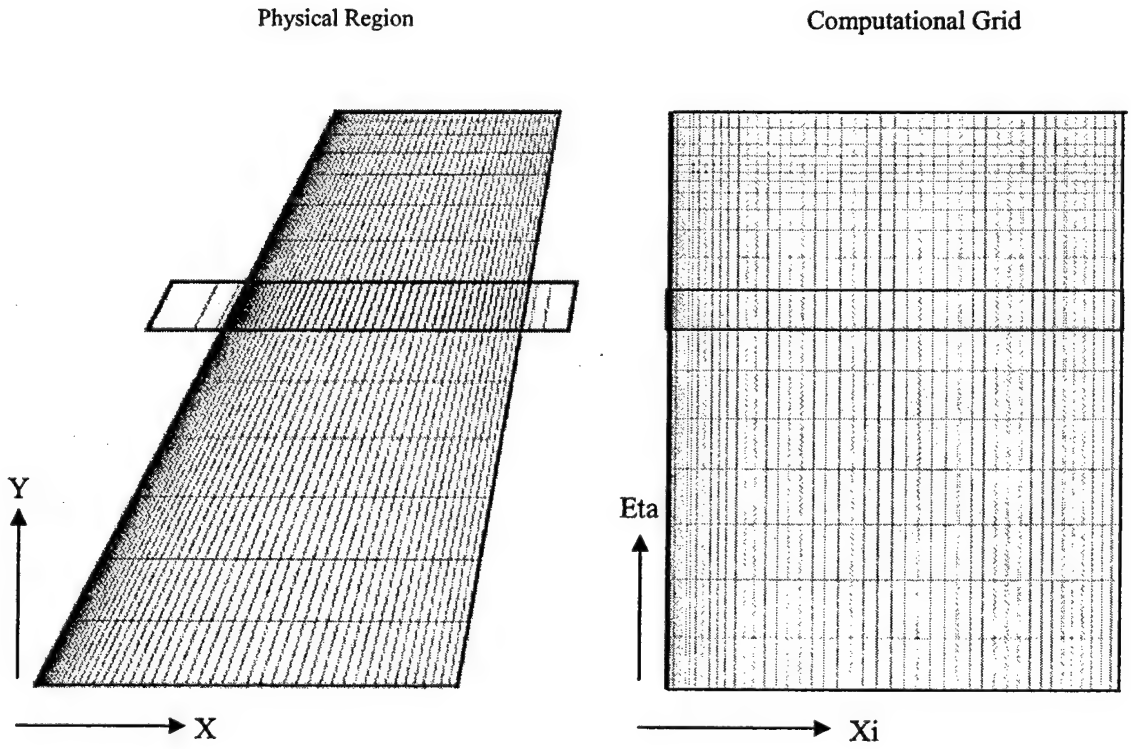

Figure 3: Aerodynamic modeling of wing and underwing store using CAP-TSD

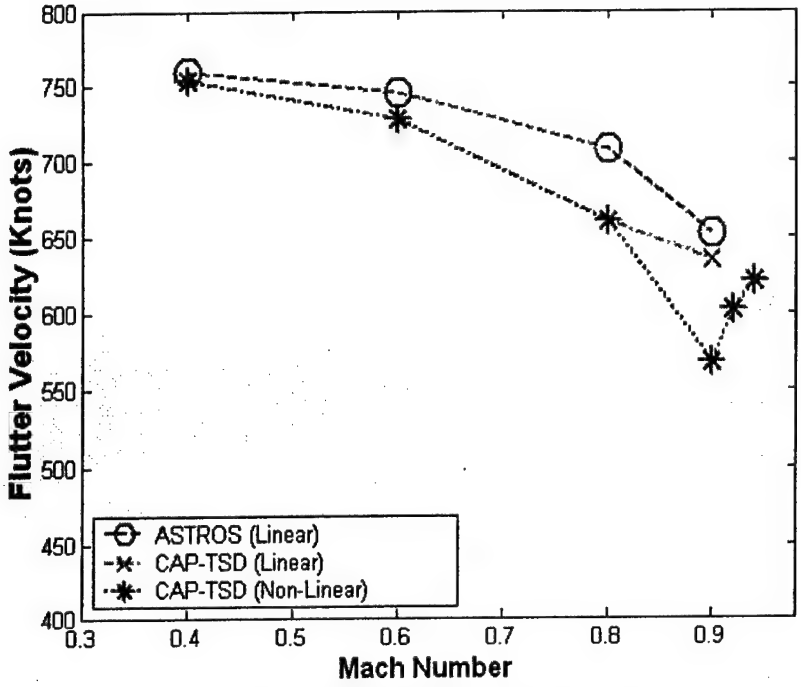

Figure 4: Flutter velocities for a clean wing

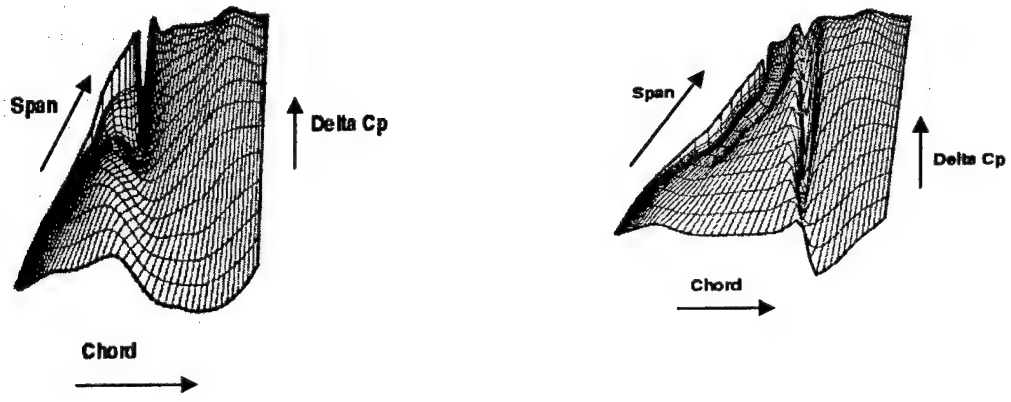

Figure 5: Unsteady Pressure Distribution - Indicating presence of shocks at Mach 0.90 and 0.92 respectively

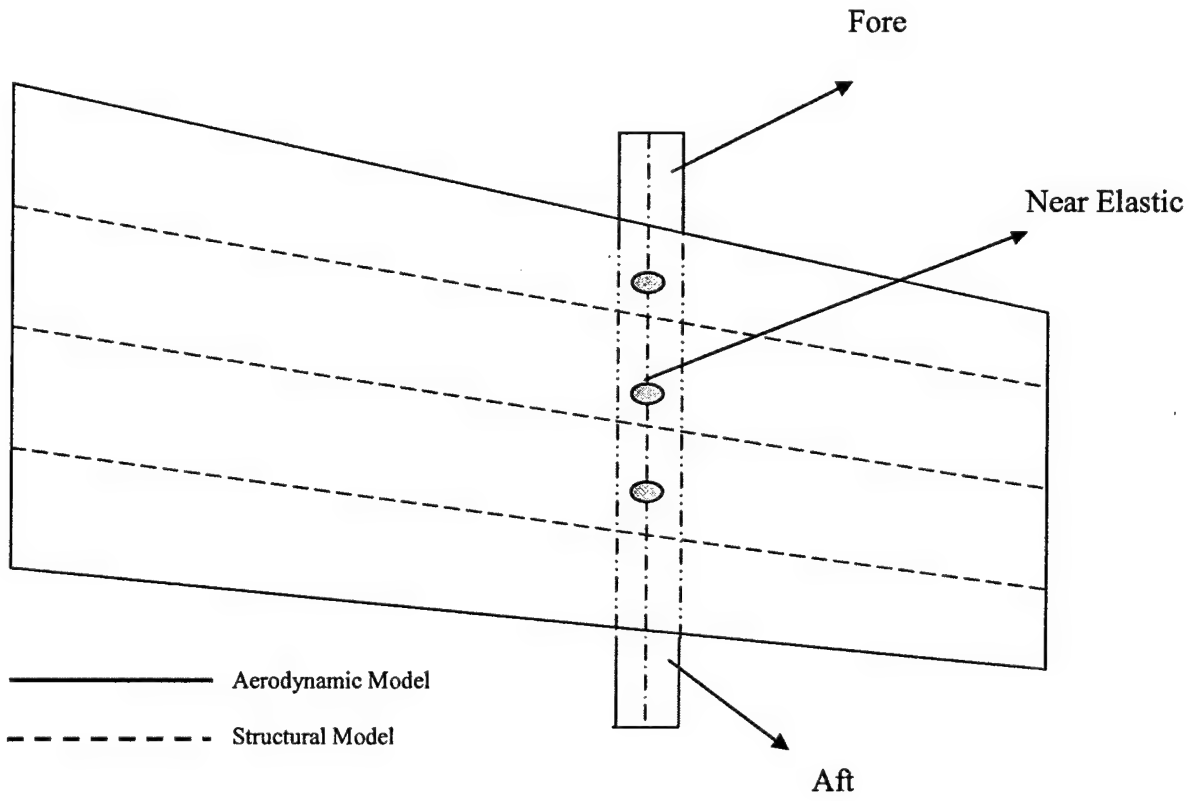

Figure 6: Center of gravity representation for
various store configurations

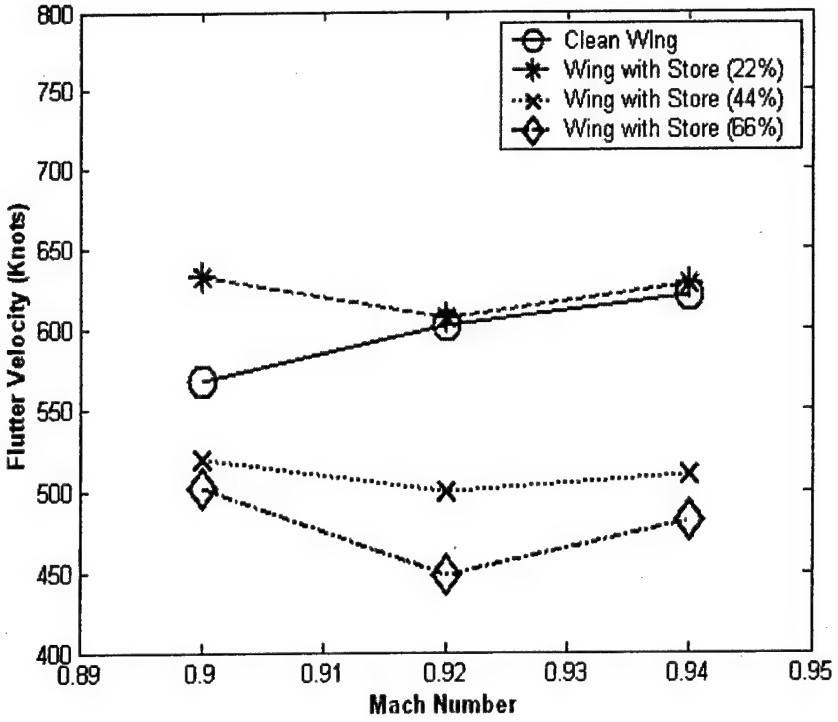

Figure 7: Sensitivity of flutter velocity to underwing store with center of gravity (mass only)

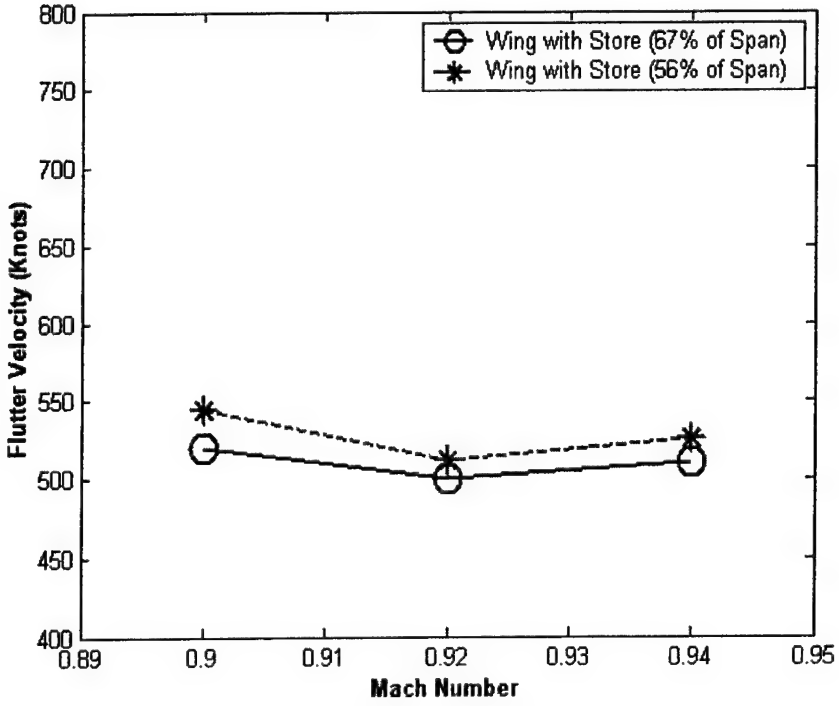

Figure 8: Sensitivity of flutter velocity to underwing store along the span of the wing (mass only) for store configuration 2

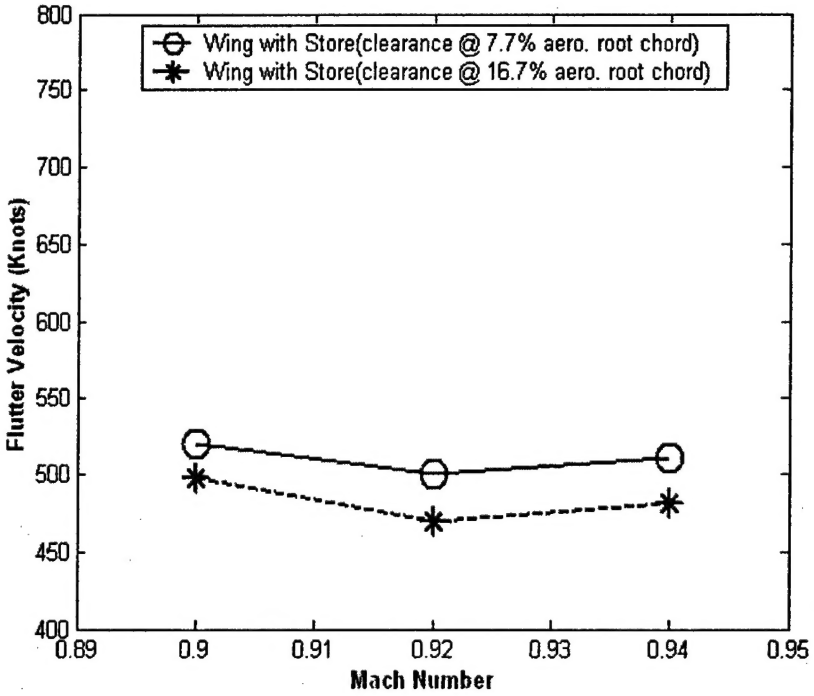

Figure 9: Sensitivity of flutter velocity to underwing store with underwing clearance (mass only) for store

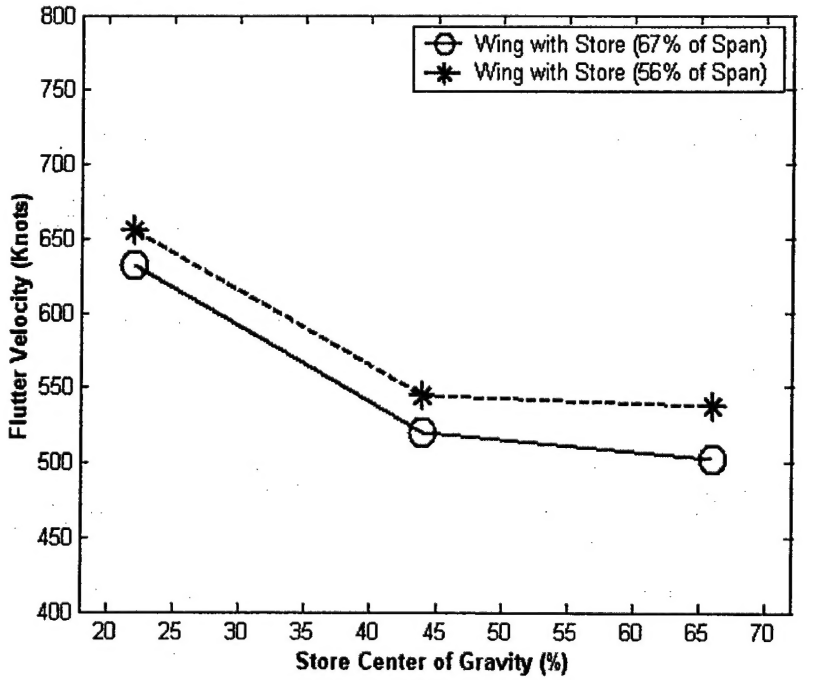

Figure 10: Sensitivity of flutter velocity to underwing store with location of span with respect to center of gravity of store (mass only)

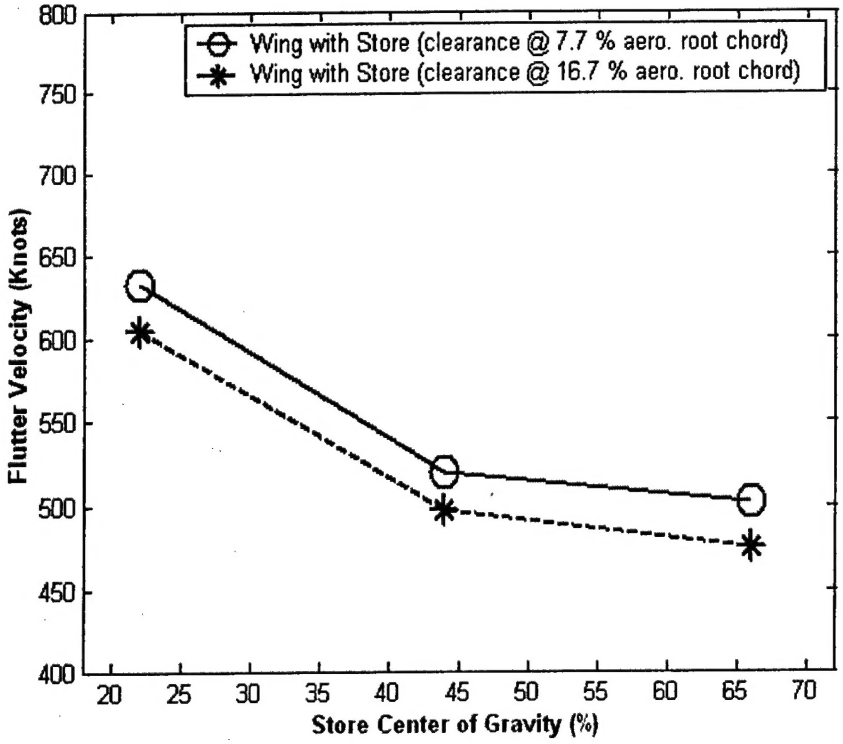

Figure 11: Sensitivity of flutter velocity to underwing store with underwing clearance with respect to center of gravity of store (mass only)

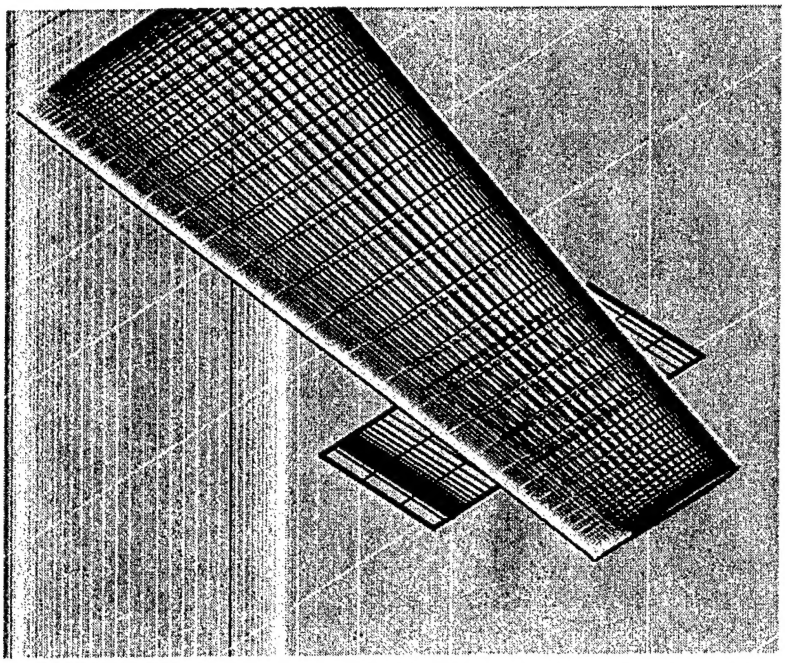

Figure 12: Aerodynamic grid of wing with underwing store using CAP-TSD

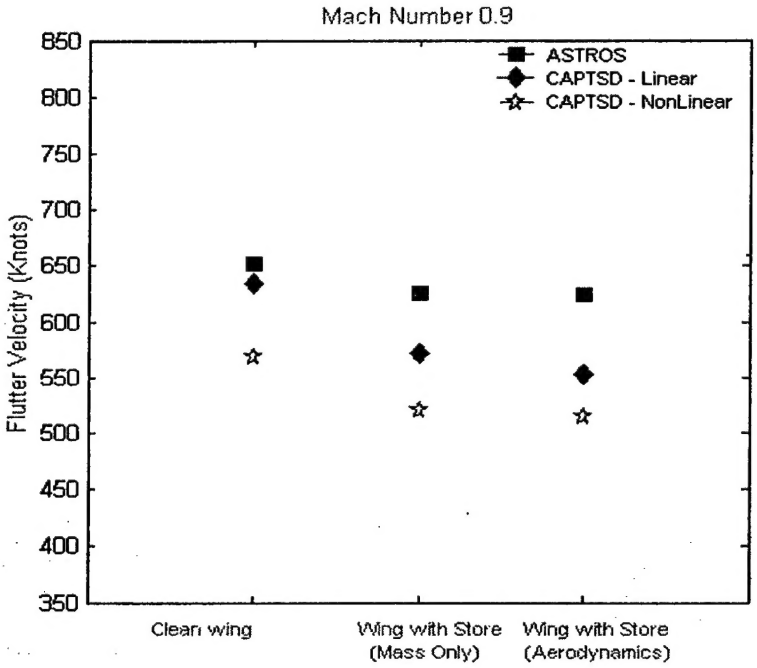

Figure 13: Comparison of flutter velocities for Linear (ASTROS), Linear (CAP-TSD) and Non-Linear (CAP-TSD) for store configuration 2

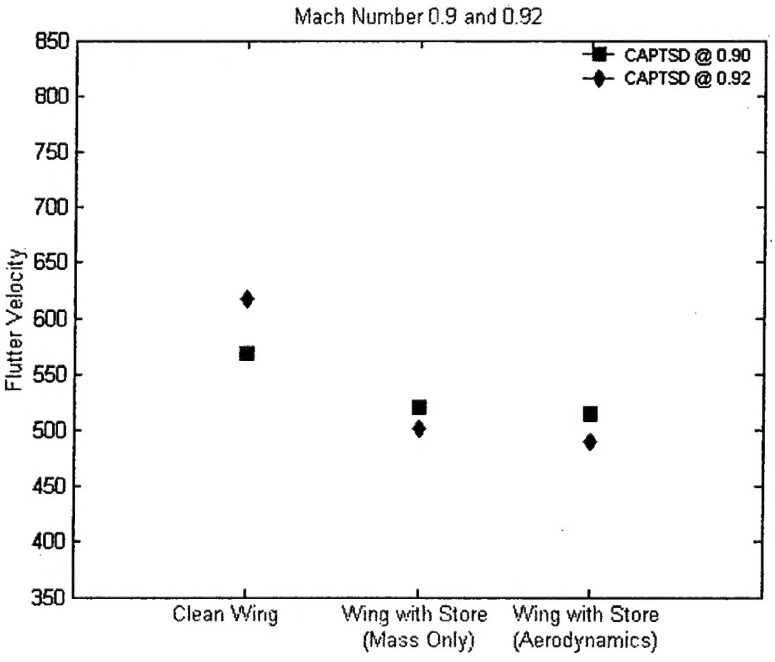

Figure 14: Comparison of flutter velocities (knots) for M=0.9 and M=0.92 using Non-Linear (CAP-TSD) for store configuration 2

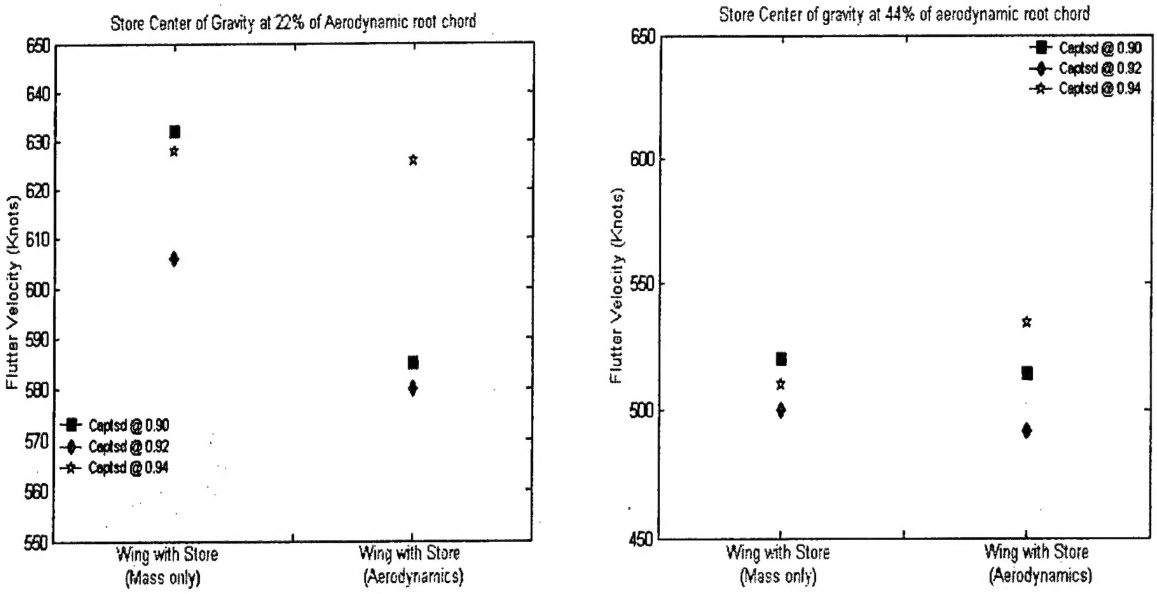

Figure 15: Comparison of flutter for store configurations 1 and 2 with and without store aerodynamics